Supporting Information

Ligase Detection Reaction Generation of Reverse Molecular Beacons for Near Real-Time Analysis of Bacterial Pathogens using Single-Pair FRET and a Cyclic Olefin Copolymer Microfluidic Chip

Zhiyong Peng[1] and Steven A. Soper[1,2,3*]

[1]Department of Chemistry and [2]Department of Mechanical Engineering

Louisiana State University, Baton Rouge, Louisiana

[3]Nano-BioTechnology and Chemical Engineering

Ulsan National Institute of Science and Technology

Ulsan, South Korea

Maneesh R. Pingle and Francis Barany

Department of Microbiology, Weill Medical College of Cornell University, New York, New York

Lloyd M. Davis

Center for Laser Applications, University of Tennessee Space Institute, Tullahoma, TN

*Author to whom correspondence should be addressed.

Conformational analysis of the rMB. As noted in the Experimental Section, the design of the reverse molecular beacon (rMB) was aided by the IDT molecular folding program to assure that the dominant conformation was indeed the closed hairpin form. The major input parameters to the analysis program included the sequence of the DNA, the salt concentration and the folding temperature. The T_m of the rMB's stem was computed by this program and possible secondary structures were generated and displayed as well. The loop sequence of the rMB was designed based on the known sequence of Gram(+) bacterial strains or to exactly match the corresponding sequence in *S. aureus* and *S. epidermidis* if strain-specificity was required. The two stem sequences were anchored to each end of the loop sequences and were designed to be complementary to each other, but not to the target. They possessed a high GC content resulting in a relatively high T_m. Therefore, the formation of the stem was thermodynamically favored over the loop-target hybrid at the concentrations employed for the LDR. At particular temperatures, the loop-target duplex and possible secondary structures associated with the rMB could coexist with the typical stem-loop hairpin structure and thus, reduce the observed FRET signal. However, at a single-molecule detection temperature of ~75ºC, the loop-target duplex was predominantly denatured and the possibilities of undesirable secondary structures of the rMB were significantly minimized. Thus, the predominant species was the rMB. Figure S1 shows a secondary structure obtained from the DNA folding program of a 63 base rMB at 75ºC in a solution buffered with 50 mM NaCl and 10 mM $MgCl_2$.

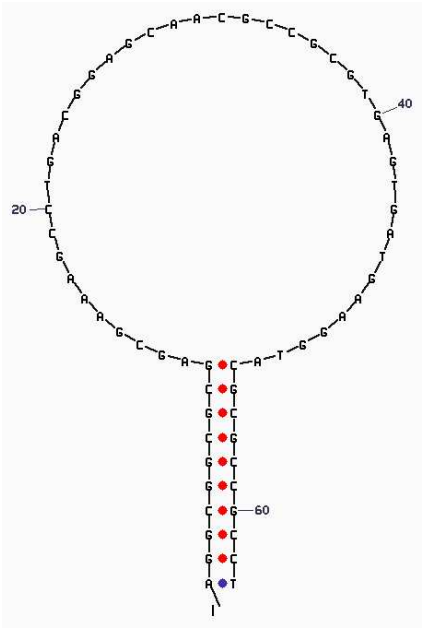

FIGURE S1. Secondary structure of a 63-base rMB folded at 75ºC. The loop sequence (43 nt) contained the reporter sequence of the particular bacteria under investigation while the stem sequence was similar for all of the rMBs used in these investigations. The loop sequence was selected to minimize any bulges formed due to secondary structure. The conformational state was determined using the IDT folding program. The T_m of the resulting stem structure for this rMB was calculated to be 83.4ºC.

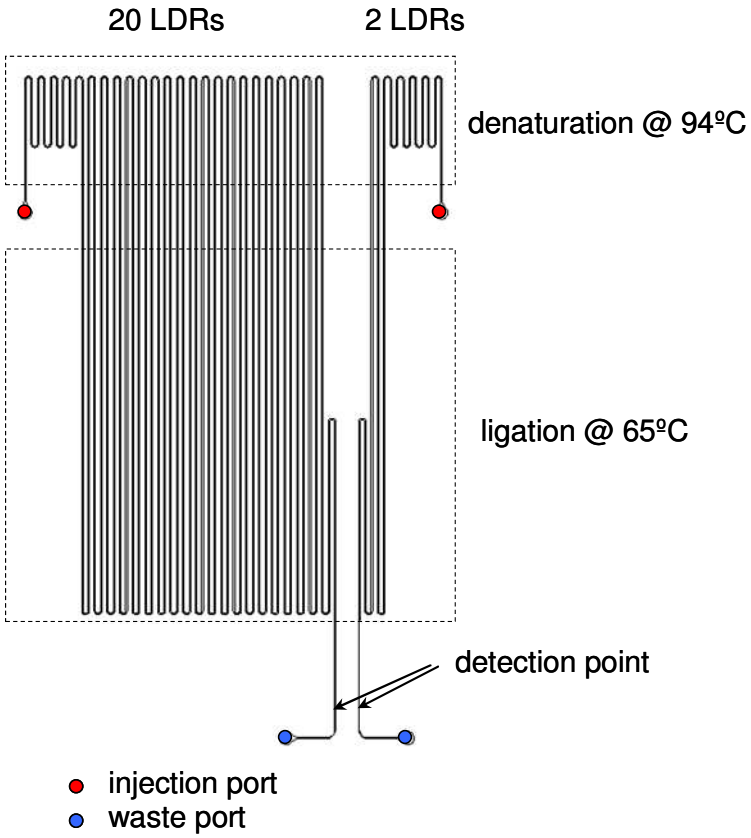

FIGURE S2. Schematic representation of the microfluidic device hot embossed from a COC substrate. The microfluidic device consisted of two different thermal reactors both of which performed LDRs in a continuous flow format.[2] One carried out 20 LDR thermal cycles (1,500 mm total length) and the other performed 2 LDR thermal cycles (total length = 204 mm). Both of the channels were 100 µm in width and 100 µm in depth. The detection window was located at the end of each channel to allow for on-chip single-molecule observation of the spFRET signals generated from the rMBs.

Fabrication of the COC microfluidic device. The microfluidic chip was fabricated using procedures developed in our laboratories,[1, 2] which involved patterning microstructures on a brass molding tool through a micro-milling process followed by transferring the microstructures into a COC substrate (Topas Advanced Polymer, Florence, KY), which has a glass transition temperature (Tg) of 130ºC, using hot embossing and a brass molding tool. COC was selected as the substrate due to its high Tg to minimize any thermally-induced structure deformation at the temperatures employed for the LDR and also, its excellent optical properties.[3, 4] The layout of the microchip architecture is shown in Figure S2. Following embossing, the COC substrate was rinsed and sonicated in isopropanol for 10 min and then in ddH_2O for 20 min. A COC cover plate was thermally fusion bonded to the embossed microchip by sandwiching the cover plate/substrate assembly between two glass plates in a convection oven and maintaining the temperature at 134ºC for 20 min. After cooling, the assembled microchip was rinsed thoroughly with ddH_2O.

The microchip was composed of two different devices, both of which performed LDRs in a continuous flow format.[2] One device contained a continuous flow thermal reactor to carry out 20 LDR thermal cycles while the other possessed only 2 LDR thermal cycles. The channels used for the thermal cycling in both devices were 100 μm in width and 100 μm in depth. At the end of each continuous flow thermal cycler device was positioned a detection region, which allowed for on-chip single-molecule observation of spFRET signals generated from the rMBs.

Operation of the microchip. A fused silica capillary (365 μm O.D.; 100 μm O.D., Polymicro Technologies, Phoenix, AZ) was inserted into the microchip and connected to a glass syringe (SGE, Australia) via a syringe-to-capillary adapter (InnovaQuartz, Phoenix, AZ). An LDR cocktail was first run through a 0.2 μm filter to remove any large particulates. Then, the reaction mixture was loaded into a glass syringe and driven by a syringe pump (Pico Plus, Harvard Apparatus, Holliston, MA) through the microchannels of the chip. Thin-film Kapton heaters were placed at the appropriate positions on the chip to provide the desired temperatures for the LDR and spFRET detection. The denaturation and renaturation/ligation zones are shown in Figure 2. A 3.5 mm gap was situated between the denaturation and renaturation/ligation zones to minimize any thermal crosstalk. The volume flow rate was set between 0.1- 4 μL/min depending on the required ligation time and also, optimizing the signal-to-noise ratio for the single-molecule measurement.

Analysis of PCR and LDR products. Five μL of each PCR product was pre-mixed with 2 μL of a loading dye and 5 μL of nuclease-free H_2O and loaded into a 3% ReadyAgarose Mini Gel (Bio-RAD, Hercules, CA). The electrophoresis was run using 1X TAE buffer and an electric field strength of 8 V/cm for 50 min. This was then followed by staining the gel with ethidium bromide for 20 min and subsequently soaking in clean H_2O for another 20 min to remove excess staining dye. The gel was then sent to a gel imaging system (Gel Logic 200, Carestream Molecular Imaging, New Haven, CT) to confirm the presence of PCR products.

To examine the fidelity and yield of the designed LDRs, these products were analyzed via capillary gel electrophoresis with laser-induced fluorescence detection (Beckman Coulter CEQ8000, Fullerton, CA). Five μL of each LDR product was loaded into different wells in a 96-well titer plate and mixed with 35 μL of loading buffer. DNA size standards were also added into a separate well. A drop of mineral oil was applied into each sample well to prevent evaporation during the thermal denaturation step. The separation buffer was added into wells of another 96-well titer plate. The LDR products were first denatured at 94ºC for 2 min and then injected into the capillary gel column using a voltage of 2 kV for 15 s. The separation was carried out using 6 kV for 30 min. The sieving gel contained denaturing additives and the capillary was maintained

at a temperature of 60ºC to ensure that the hairpin structure of the LDR product was fully opened during the electrophoretic separation.

Generating test targets for LDR using PCR amplified genomic DNA. To initially evaluate the efficiency of the spFRET assay using LDR from genomic bacterial DNA, we carefully controlled the copy number of DNA targets included in the assay and used PCR amplicons as the input (see Table 1 for PCR primer sequences), which was generated from all bacterial species and the subsequent LDRs were carried out using these PCR amplicons. The primer set AMP1 (see Table 1), was designed to produce a 388 bp amplicon from the 16S rRNA gene for each species in order to produce test targets for evaluating the efficiency of the LDR spFRET assay. Ten ng of genomic DNA from each bacterial species were used as the targets for the amplification.

After 35 PCR cycles, the products were validated by running agarose gel electrophoresis. Two different primer sets were used for the PCR, AMP1 and/or AMP2 (see Table 1 for sequences), in which the AMP1 primer set produced a 388 bp amplicon. Primer set AMP2 was designed to produce a 423 bp amplicon from a different region of the 16S rRNA gene. Figure S3 shows the 388 bp amplicons (lanes B, C, D) and the 423 bp amplicons (lanes E, F, G) when primer set AMP1 or AMP2 were used, respectively. From this data, successful amplification of the target sequences was secured using all bacterial species. These regions of the genome were then interrogated via LDR to provide information on the Gram(+) or Gram(-) status of the target and/or determining its strain. A multiplexed PCR was also performed where both primer sets were added into the same reaction cocktail. Lanes H, I, J in Figure S3 shows the presence of two amplicons with different lengths for *S. aureus*, *S. epidermidis* and *E. coli*.

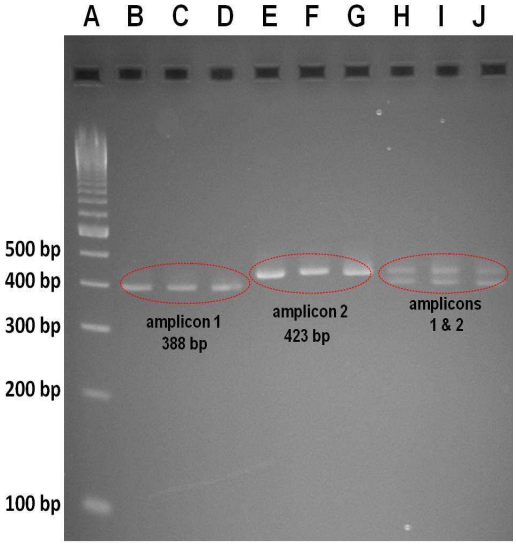

FIGURE S3. Gel electrophoresis images of dsDNA PCR products along with a sizing ladder. Electrophoresis were run using primer set AMP1 and/or AMP2 to amplify two different regions of the 16S rRNA gene for *S. aureus*, *S. epidermidis* differentiation. Lanes A = sizing ladder; B = *S. aureus* (AMP1); C = *S. epidermidis* (AMP1); D = *E. coli* (AMP1); E = *S. aureus* (AMP2); F = *S. epidermidis* (AMP2); G = *E. coli* (AMP2); H = *S. aureus* (AMP1 + AMP2); I = *S. epidermidis* (AMP1 + AMP2); J = *E. coli* (AMP1 + AMP2). A 388 bp amplicon was generated when primer set AMP1 was employed in the PCR and a 423 bp amplicon was formed when primer set AMP2 was used. The PCR was run for 35 thermal cycles at 94ºC for 15 s, 60ºC for 1 min, 72ºC for 1 min, and a final extension at 72ºC for 7 min. The PCR products were separated using a 3% ReadyAgarose Mini Gel. The electrophoresis was run in 1X TAE buffer under an electrical field of 8 V/cm for 50 min.

Effects of linker structure on FRET efficiency. We also investigated different linker structures to assess their impact on the efficiency of energy transfer. The different linker structures evaluated are shown in Table S1. The cyanine dye molecules, Cy5 and Cy5.5, were attached to either the 5' or 3' terminus of the oligonucleotides used for the LDR employing either a 3-carbon, 6-carbon, or 9-carbon linker structure, which provided different effective lengths between the donor/acceptor dyes based on molecular structure considerations.

Table S1. Different linker structures used for dye-labeling of the LDR primers.

Primers	Size	Sequence
discriminating	30	5' Cy5.5-C3-AGGCGGCGCGAGCGAAAGCCTGACGGAGCA 3'
discriminating	30	5' Cy5.5-C9-AGGCGGCGCGAGCGAAAGCCTGACGGAGCA 3'
common	33	5' pACGCCGCGTGAGTGATGAAGGTACGCGCCGCCT-C3-Cy5 3'
common	33	5' pACGCCGCGTGAGTGATGAAGGTACGCGCCGCCT-C6-Cy5 3'

Different polymer substrates for the microfluidic. We were also interested in deciding which polymer would be optimal for the fluidic chip. The requirements for this selection included; (i) the material must be easily molded into the desired structures using hot embossing; (ii) biocompatibility (provide highly efficient yields of the LDRs); and (iii) demonstrate low levels of autofluorescence to produce high signal-to-noise ratios for the single-molecule detection. Table S2 shows the autofluorescence levels produced from three different thermoplastics. As can be seen, COC produced the lowest background fluorescence of the three materials investigated. We also found that COC was able to provide highly efficient LDR yields as well (data not shown). In addition, its high Tg provided good microstructure integrity when heated zones were applied to the chip for the LDR. Therefore, this material was used throughout these studies.

Table S2. Autofluorescence of commonly used thermoplastic materials used for microfluidic applications.

Thermoplastic Material	Dimension of Microchannel	Fluorescence Background
Poly(methyl methacrylate) (PMMA)	100 x 100 µm	~ 5,000 counts/s
Polycarbonate (PC)	100 x 100 µm	~ 40,000 counts/s
Cyclic Olefin Copolymer (COC)	100 x 100 µm	~ 1,000 counts/s

*The measurement was carried using the laser-induced fluorescence system described in this manuscript. Each polymer was molded via hot embossing to form microchannels. All three chips were then thermally fusion bonded to a 100 µm thick cover plate made from the same material as the substrate. The fluidic channel was filled with 1X TBE buffer prior to the measurement.

Verifying successful LDRs. PCR products from *S. aureus*, *S. epidermidis* and *E. coli* were quantified by UV absorption at 260 nm and diluted to the required concentration, which were then used as targets for LDR. To validate the appropriate LDR products were indeed generated and to determine LDR efficiency, the LDR products were subjected to capillary gel

electrophoresis. Figure S4 (A) shows a capillary gel electrophoretic analysis of LDR products generated following 20 thermal cycles with 10 nM of each primer and 1 nM of the PCR product secured from *S. aureus*. In the electropherogram, the peaks that eluted early in the electropherogram resulted from unligated primers. Size standards, which consisted of equal amounts of a 13 base and 88 base single-stranded oligonucleotides were co-electrophoresed with the LDR products and used for the size determination. From Figure S4, it can be seen that the two primers were successfully ligated to form a 63 base oligonucleotide, the designed length of the rMB. The magnitude of the peaks associated with the shorter (unligated primers) and longer (ligated primers) fragments also provided information as to the relative amounts of these two fragments from which the efficiency of the ligation reaction could be evaluated. In this example, the ratio of the peak height of the LDR products to the peak height of the primers was 3.96, indicating a concentration of ~8 nM for the LDR products and 2 nM for the unligated primers. Considering that 100% LDR efficiency for each thermal cycle would result in 1 nM of product, the average reaction efficiency was determined to be 40% for each LDR cycle.

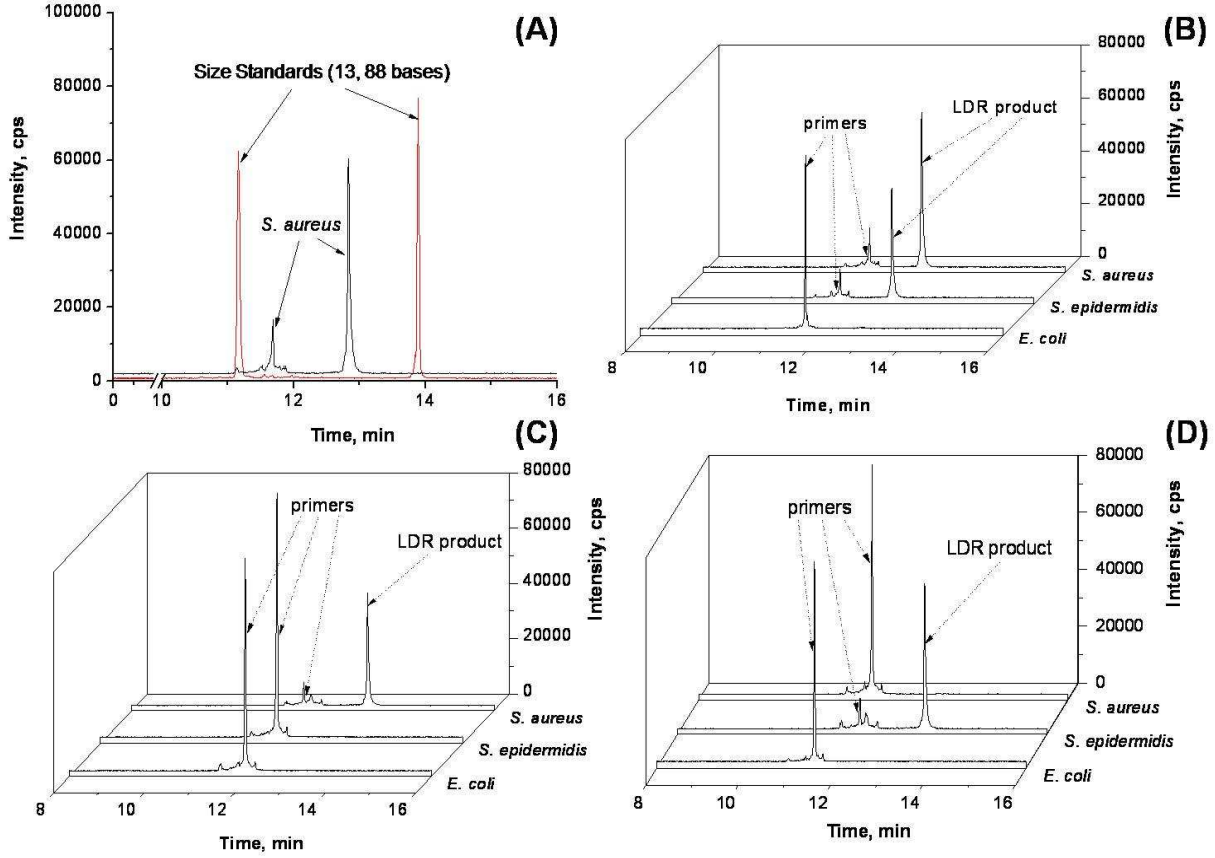

FIGURE S4. Electropherograms of LDR products from different bacterial samples. (A) LDR products from *S. aureus* amplicons (black) and the size standards (red). The size standards contained roughly equal amounts of a 13 nt and 88 nt single-stranded DNA fragment. (B) LDR products generated using the primer set specific for Gram(+) bacteria to allow differentiation between Gram(+) and Gram(-) strains. (C) LDR products generated using *S. aureus* specific LDR primers. (D) LDR products using *S. epidermidis* specific LDR primers. For all electropherograms, the LDR was run for 20 cycles at 94ºC for 30 s and 65ºC for 2 min using a bench-top thermal cycler. The LDR cocktail contained 10 nM of each primer and 1 nM of the PCR product from different bacterial samples. LDR products were analyzed via capillary gel electrophoresis equipped with laser-induced fluorescence detection. The sample was denatured at 94ºC for 2 min and then injected into the capillary using a voltage of 2 kV for 15 s. The separation was carried out using a voltage of 6 kV for 30 min.

References

(1) Wang, H.; Chen, J. F.; Zhu, L.; Shadpour, H.; Hupert, M. L.; Soper, S. A. *Analytical Chemistry* **2006**, *78*, 6223-6231.

(2) Hashimoto, M.; Barany, F.; Soper, S. A. *Biosensors & Bioelectronics* **2006**, *21*, 1915-1923.

(3) Pu, Q. S.; Oyesanya, O.; Thompson, B.; Liu, S. T.; Alvarez, J. C. *Langmuir* **2007**, *23*, 1577-1583.

(4) Steigert, J.; Haeberle, S.; Brenner, T.; Muller, C.; Steinert, C. P.; Koltay, P.; Gottschlich, N.; Reinecke, H.; Ruhe, J.; Zengerle, R.; Ducree, J. *Journal of Micromechanics and Microengineering* **2007**, *17*, 333-341.